ADVANCED MATERIALS

DOI: 10.1002/adma.200702221

Fabrication of Luminescent Nanoarchitectures by Electron Irradiation of Polystyrene**

By *Hyeok Moo Lee, Yong Nam Kim, Bong Hoon Kim, Sang Ouk Kim,* and *Sung Oh Cho**

Light-emitting nanostructures are widely used for optical, photonic, chemical, and biological devices.[1–4] For example, fluorescent nanoparticles are useful for biological assays,[5] chemical sensors,[6] and organic lasers,[7] whereas one-dimensional luminescent nanowires are exploited for novel nanoscale photonic devices such as nanolasers[8] and nanowire scanning microscopy.[1] Rapid progress in nanoscale devices requires well-defined luminescent nanoarchitectures. Several methods to prepare organic, inorganic, and polymeric light-emitting nanostructures have been developed.[9–13] However, fabrication of luminescent nanoarchitectures with a tailored morphology and pattern is still challenging. Here we present a straightforward strategy to produce desired luminescent nanoarchitectures and nanopatterns by electron irradiation of a polystyrene (PS) homopolymer. We have discovered that non-luminescent polystyrene can be converted into a luminescent organic material, the emitting color of which can be tuned by electron irradiation. Based on this fact, we demonstrate that luminescent nanopatterns can be readily fabricated only by irradiating selected regions of PS by an electron beam. In addition, the top-down irradiation approach in conjunction with self-assembled PS nanostructures allows fabrication of diverse and complex luminescent nanoarchitectures.

PS consists of long hydrocarbon chains with an aromatic ring in the repeating unit. Although conjugated carbon units exist in the monocyclic ring, PS does not exhibit luminescence in the visible spectral region.[14] Interestingly, however, we discovered that PS emitted intense visible light when the polymer was irradiated with an electron beam: PS films spun on Si substrates were irradiated under vacuum with a 50 keV electron beam.[15] Electron-irradiated PS also exhibited photoluminescence (PL) at room temperature (Fig. 1). PS irradiated at a relatively low electron dose of 272 $\mu C\ cm^{-2}$ displayed blue PL when excited with ultraviolet (UV) light at a wavelength of 325 nm. The blue PL spectrum had a peak at 395 nm with a full width at half maximum (FWHM) of 69 nm. As the electron dose increased, the PL peak red-shifted and the FWHM of the peak increased. When the electron dose was increased to 15.2 $mC\ cm^{-2}$, the PL spectrum of the irradiated PS under the UV excitation covered the full visible spectral region; the PL peak was centered at 505 nm with a FWHM of 165 nm, resulting in white emission color. Therefore, luminescent materials with tunable emitting color can be obtained by merely irradiating PS homopolymer with an electron beam.

To elucidate the origin of the visible luminescence from electron-irradiated PS, we characterized the optical properties and the chemical structures of PS samples by UV-vis, ^1H NMR, and attenuated total reflection Fourier transform infrared (ATR-FTIR) spectroscopy. UV-vis absorption spectra of irradiated PS samples showed that the absorption edge red-shifted from UV toward visible as the electron dose was increased (Fig. 2a). Moreover, the optical bandgap (Tauc gap)[16] of the irradiated sample decreased with increasing the electron dose (inset of Fig. 2a). These phenomena suggest that conjugated carbon units in the form of olefinic chains or aromatic rings are generated in irradiated PS and that the conjugation length increases as a function of the electron dose.[17] ^1H NMR spectra of PS samples are shown in Figure 2b. Irradiated PS became more insoluble in the solvent with increasing the electron dose, allowing clear NMR spectra only for the PS samples irradiated at a comparatively low electron dose ($<\sim 3.2\ mC\ cm^{-2}$). The NMR spectrum of an irradiated PS sample, in contrast to pristine PS samples, displayed new resonance peaks in the range of 7.4 to 8.7 ppm, indicating that polycyclic aromatic hydrocarbons (PAHs)[18] such as biphenyl, *p*-terphenyl, substituted naphthalene, and phenanthrene were created in the irradiated PS (see details in Fig. 2b). PAHs that consist of multi aromatic rings show interesting lumine-scence properties because of the cyclic conjugated structure of the aromatic rings.[19] The optical bandgaps (E_g) of PAHs are determined by the number of clustered aromatic rings (M) by the relationship $E_g \approx 6/\sqrt{M}$ eV,[16] which explains that the luminescence spectra of PAHs red-shift with an increase in cluster size. On the other hand, no resonance peaks corresponding to olefinic compounds were observed in both ^1H NMR and ATR-FTIR spectra (Fig. 2c) of irradiated PS specimens. Therefore, it is reasonable to conclude that the luminescence of irradiated PS is attributed to PAHs generated by electron irradiation.

[*] Prof.S. O. Cho, H. M. Lee, Y. N. Kim
Department of Nuclear and Quantum Engineering
Korea Advanced Institute of Science and Technology
Daejon 305-701 (Korea)
E-mail: socho@kaist.ac.kr
B. H. Kim, Prof.S. O. Kim
Department of Materials Science and Engineering
Korea Advanced Institute of Science and Technology
Daejon 305-701 (Korea)

[**] This work was supported by a Korea Science and Engineering Foundation (KOSEF) grant funded by the Korea government (MOST) (No. 2007-00543). Supporting Information is available online from Wiley InterScience or from the authors.

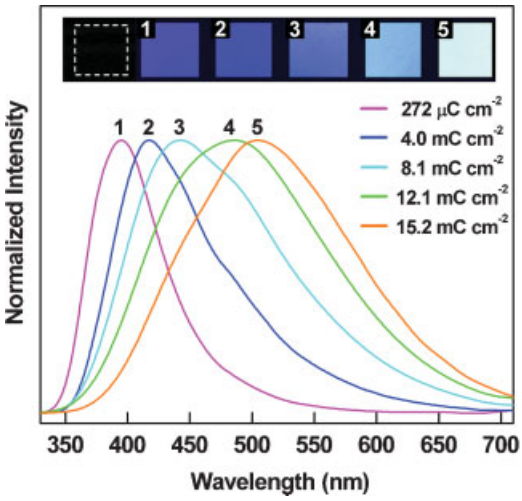

Figure 1. Room-temperature photoluminescence characteristics of irradiated PS as a function of electron dose. The emission spectra were measured with the 325 nm line of a Xe lamp as excitation source. The upper inset shows fluorescence microscopy images of the irradiated samples under excitation of UV light. The dashed box in the inset corresponds to a non-irradiated PS sample, showing no luminescence.

Analysis of ATR-FTIR spectra helps to reveal the formation process of PAHs. The FTIR spectra show that aromatic C–H bonds of PS are rapidly decomposed by electron irradiation, whereas sp^2 C=C bonds of aromatic rings are almost intact under the irradiation (Fig. 2c). This suggests that aryl radicals are abundantly formed in irradiated PS. Electron irradiation also dissociates aliphatic C–H bonds, backbone C–C, and pendant groups,[18,20] leading to the formation of various radicals, including main chain radicals, chain-end radicals, and phenyl radicals. These radicals can make bonds with each other to form new molecular structures. For example, crosslinking of aryl radicals on different chains produces non-fused PAHs such as biphenyl and terphenyl. Reactions between aryl radicals and chain radicals result in fused PAHs such as phenanthrene (see details in Supporting Information, Fig. S1). The created PAHs can grow through subsequent interactions with other radicals. Consequently, as the electron dose increases, the PS polymer is gradually transformed to an organic network structure that is mainly composed of fused and non-fused PAHs with different cluster sizes. Furthermore, the average cluster size of the generated PAHs increases with increasing the electron dose.

The fact that non-luminescent PS can emit blue or white light by electron irradiation can be used for many interesting applications. In particular, PS can be prepared with well-defined nanoarchitectures using many bottom-up approaches. Then, only by irradiating the prepared polymer with an electron beam, luminescent nanoarchitectures that keep pristine morphologies can be produced. To demonstrate this, we prepared a regularly ordered colloidal crystal by self-assembly of PS nanospheres (diameter: 350 nm)[21] and subsequently irradiated the colloidal crystal with an electron

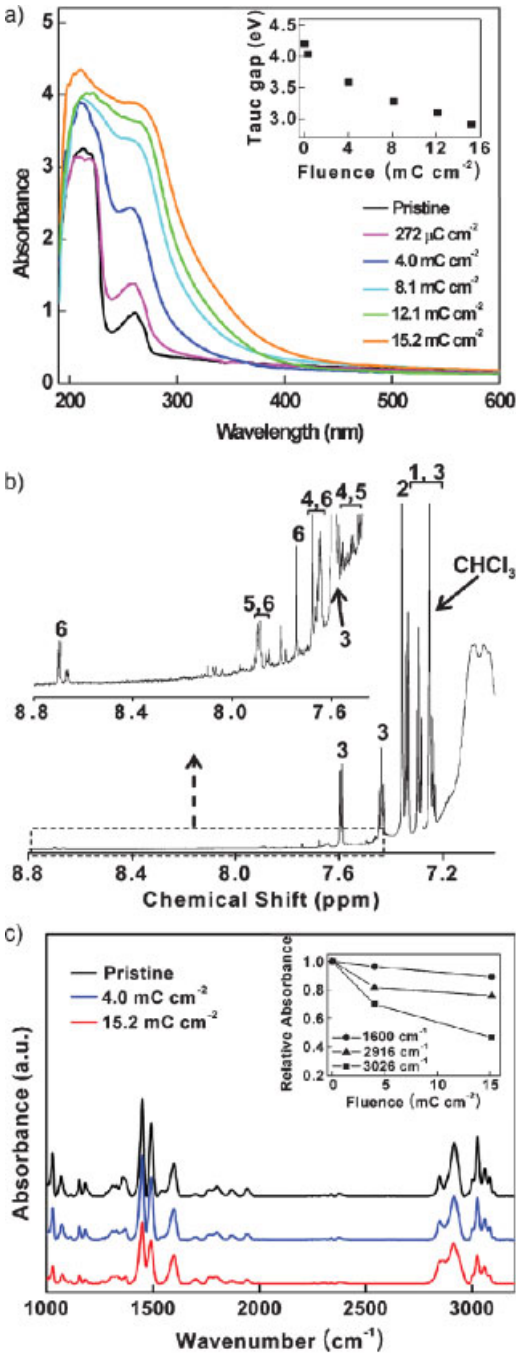

Figure 2. Characterization of PS samples. a) UV-vis absorption spectra of both a pristine PS sample and electron-irradiated PS samples at different electron doses. The inset is Tauc optical gap of the PS samples as a function of electron dose. b) ^{1}H NMR spectra of a pristine PS and electron-irradiated PS samples. The inset is magnified NMR spectra in down-field region. The resonance peaks are assigned to 1: phenyl derivatives, 2: benzene, 3: biphenyl, 4:*p*-terphenyl, 5:1-phenylnaphthalene, and 6: phenanthrene, respectively. c) ATR-FTIR spectra of the PS samples at different electron dose. Important vibration bands lie at 1600 cm^{-1} (aromatic C=C stretching), 2800–3000 cm^{-1} (aliphatic C–H stretching), and 3000–3100 cm^{-1} (aromatic C–H stretching). The inset shows relative optical densities of the major peaks of the irradiated PS compared to those of the pristine PS. No new peak at 1640 cm^{-1} corresponding to olefinic C=C stretching appeared.

ADVANCED MATERIALS

beam. As shown in the scanning electron microscopy (SEM) and cathodoluminescence (CL) images, each of the irradiated PS nanospheres emitted visible light while preserving the pristine colloidal crystal structure (Fig. 3a and b). Luminescent PS spheres can be dispersed in water and, thus, individual light-emitting particles with different emission colors were also produced (Fig. S2). Luminescent nano- and microparticles are generally fabricated by incorporating fluorescent materials, such as dyes and quantum dots, into non-emissive particles.[5,22] The results shown in Figures 3b and S2 suggest that the irradiation strategy allows a simple fabrication of diverse luminescent architectures, ranging from individual light-emitting particles to 3D photonic crystals consisting of luminescent nanoparticles. Moreover, a periodic array of emissive nanowires (lateral width: 25 nm) was fabricated through electron irradiation of a symmetric poly(styrene)-*block*-poly(methyl methacrylate) (PS-*b*-PMMA) that formed self-assembled lamellar structures (Fig. 3c and d). The aligned lamellar structure was prepared by the directional growth of ordered block copolymer domain.[23,24] Because PMMA is a radiation-degrading polymer, it can be removed from the copolymer by electron irradiation in vacuum,[25] leaving PS that turns into emissive materials. As a result, such a unique luminescent nanowire array was generated by electron irradiation.

In addition, this strategy allows fabrication of desired light emission patterns by irradiating selective regions of PS films with an electron beam. Figure 4a and b displays patterned array of luminescent nanodots (dot size: 100 nm) and nanowires (lateral width: 100 nm). The luminescent nanostructures were fabricated by a direct electron-beam writing process, where an electron beam focused down to a few nanometers was scanned across a PS film to form the luminescent patterns. As described earlier PS, which is soluble in solvents such as chlorobenzene and toluene, is converted into an insoluble and luminescent organic material by electron irradiation, whereas non-irradiated regions of the PS film can be easily removed by a solvent. Thus, only luminescent layers can be left on a substrate in a similar way to negative electron-resist polymers,[26] as shown in the atomic force microscopy (AFM) topography images (insets of Fig. 4a and b). Furthermore, we fabricated a luminescent array of nanowires that were aligned on a Si substrate. Fluorescent microscope images of the nanowire arrays were shown in Figure 4c and d. The nanowire arrays were also produced by electron-beam writing on a PS film, followed by removing the non-irradiated regions of the PS film by a solvent (Fig. S3). However, thicker PS films were used for the fabrication of nanowire arrays (thickness: 12 μm in Fig. 4c and 5 μm in Fig. 4d) than for the formation of the nanodot array shown in Figure 4a (thickness: 200 nm) Hence, nanowires with high aspect ratios, instead of nanodots, were formed on the substrate. Figure 4e shows fluorescence microscopy images of various light-emitting structures, including a rose, hexagonal microrings, and circular micropores. Moreover, patterned luminescent structures can also be fabricated by using a metallic mask. Only electrons that pass through the mask irradiate and correspondingly convert PS into a light-emitting material, leading to a luminescent pattern. An array of

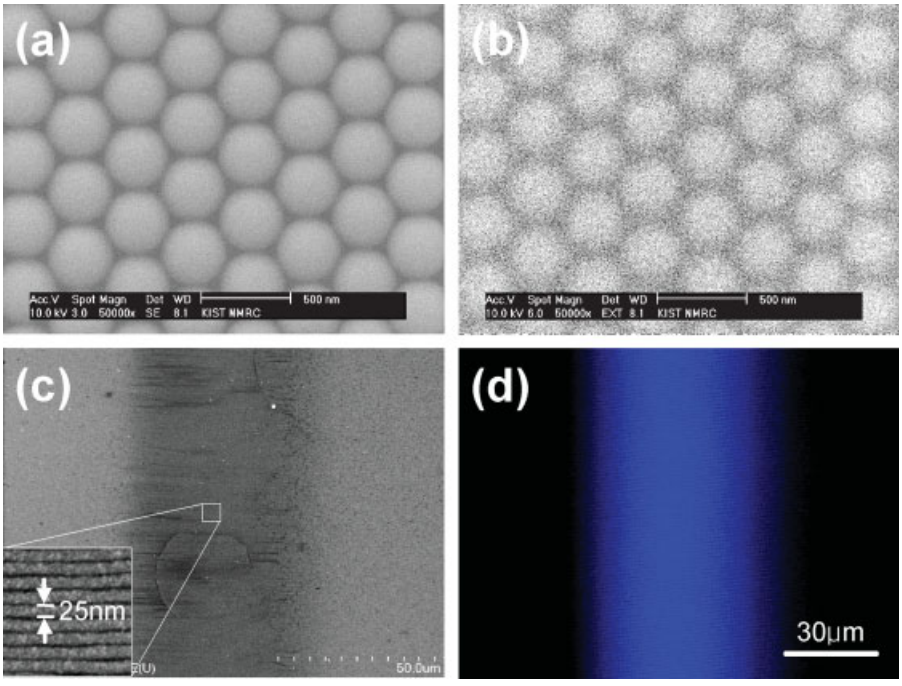

Figure 3. Arrays of luminescent polymer nanostructures. a) SEM image of a monolayer colloidal crystal self-assembled from 350 nm PS nanospheres. b) CL image from the electron-irradiated PS colloidal crystals. c) SEM image of a self-assembled PS-poly(methyl methacrylate) (PS-PMMA) lamellar structure. The lower inset is a magnified SEM image of the localized rectangular region of the lamella structure marked in the image. d) Fluorescence microscopy image of the electron-irradiated lamella structure.

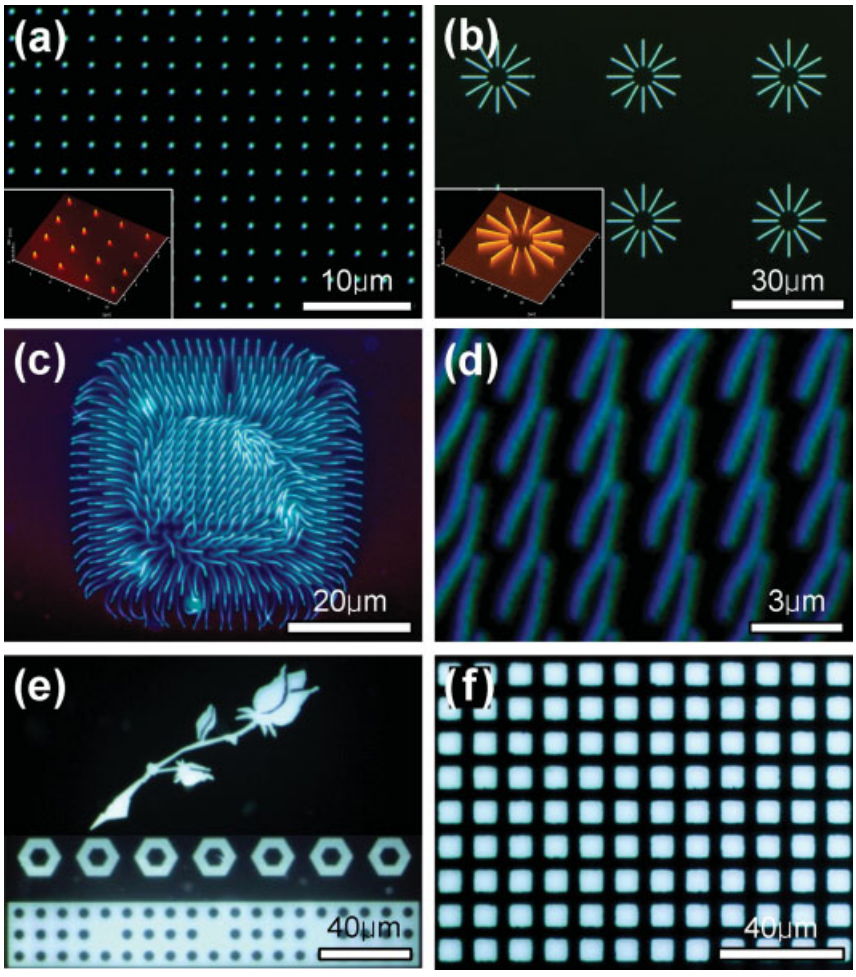

Figure 4. Patterned light-emitting nanostructures and microstructures. Fluorescence microscopy images of a) luminescent nanodots (diameter: ~100 nm) and b) nanowires (lateral width: ~100 nm) arrays. The insets are AFM topography images of the nanodot and nanowire arrays, respectively. c) Assembly of luminescent nanowires. The lateral width of the nanowires is 200 nm and the length of the nanowires is 12 μm. d) Array of luminescent nanowires aligned on a Si substrate. The nanowires have a lateral width of 200 nm and a length of 5 μm, respectively. e) Fluorescence microscopy images of light-emitting microstructures with diverse morphologies such as a rose, hexagonal microrings, and circular micropores. f) Light emissive pixel arrays patterned using a 2000-mesh copper grid as a mask.

luminescent pixels (pixel size: $7 \times 7\ \mu m^2$) shown in Figure 4f was prepared using a 2000-mesh copper grid as a mask. Consequently, the results shown in Figure 4 indicate that luminescent micro- and nanoarchitectures of arbitrary shapes and patterns can be created by the electron irradiation approach. In addition, the emission stability of electron-irradiated PS against thermal- and photo-oxidation was investigated in comparison with poly(9,9-dioctylfluorenyl-2,7-diyl) (PFO), which is known as a stable blue light-emitting polymer.[27] The measurement results (Fig. S4) indicate that irradiated PS, possibly due to PAHs, has much higher thermal- and photo-oxidative stability than PFO. This superior emission stability is attractive for the long-life performance of devices.

We have presented a strategy to obtain luminescent nanoarchitectures based on a simple one-step electron irradiation process. Electron irradiation produces light-emitting materials from non-luminescent polymers while simultaneously patterning the polymer to form nanostructures. The top-down irradiation strategy, through combination with bottom-up approaches for precursor preparation or through direct electron-beam writing, provides a powerful tool to fabricate desired complex luminescent nanoarchitectures and nanopatterns. The strategy utilizes solution-processable polymeric material as a precursor and the polymer surface can be easily functionalized to respond to chemical, biological, electronic, and optical stimuli. Therefore, we believe that the approach presented here will be useful for a wide range of research fields including optics, photonics, chemistry, and biology.

Experimental

PS films were prepared by spin-coating PS ($M_w = 2500$–200000 g mol^{-1}) dissolved in chlorobenzene on Si substrates. Electron irradiation experiments were carried out in a vacuum chamber under a pressure of less than 2×10^{-5} Torr (1 Torr $= 1.333 \times 10^2$ Pa) using a

ADVANCED MATERIALS

thermionic electron gun equipped with a tantalum cathode. The energy of the electron beam was 50 keV and the beam current density was 5 μA cm^{-2}, respectively. The electron dose was changed by controlling the irradiation time. The substrate was cooled down to prevent thermal degradation of PS. In addition, micro- and nanoscale luminescence patterns were prepared with a 100 keV electron-beam lithography system (Elionix, ELS-7000). PL spectra were recorded at room temperature using a spectrometer (PSI, DARSA PRO 5100) with the 325 nm line of a xenon lamp as the excitation source. Fluorescence images of irradiated PS film were captured using a fluorescence microscope (Olympus BX51). The excitation wavelength of the fluorescent microscope was 350–380 nm. Scanning electron microscopy (SEM) images were obtained using field-emission SEMs (Phillips FEI XL30 and Hitachi S-4800).

Cathodoluminescence (CL) images were captured by a Phillips SEM equipped with a Gatan mono CL system. AFM images were acquired by a Seiko SPA300HV. UV-vis spectra were recorded on a Shimadzu UV-3101PC spectrometer. The Tauc optical gap was determined from the UV-vis transmission and reflection spectra for the samples using the Tauc relation. ATR-FTIR spectra were measured with a Bruker IFS66V/S spectrometer coupled with a HYPERION 3000 microscope. ^{1}H NMR spectra were recorded in $CDCl_3$ at 22 °C using a Bruker Biospin AvanceII 900 spectrometer at 900MHz.

Received: September 3, 2007
Revised: January 14, 2008
Published online: May 5, 2008

[1] Y. Nakayama, P. J. Pauzauskie, A. Radenovic, R. M. Onorato, R. J. Saykally, J. Liphardt, P. Yang, *Nature* **2007**, *447*, 1098.
[2] P. Michler, A. Kiraz, C. Becher, W. V. Schoenfeld, P. M. Petroff, L. Zhang, E. Hu, A. Imamoğlu, *Science* **2000**, *290*, 2282.
[3] M. D. McGehee, A. J. Heeger, *Adv. Mater.* **2000**, *12*, 1655.
[4] J. Jang, *Adv. Polym. Sci.* **2006**, *199*, 189.
[5] M. Han, X. Gao, J. Z. Su, S. Nie, *Nat. Biotechnol.* **2001**, *19*, 631.
[6] L. Chen, D. W. McBranch, H. L. Wang, R. Helgeson, F. Wudi, D. G. Whitten, *Proc. Natl. Acad. Sci. USA* **1999**, *96*, 12287.
[7] Y. Chen, Z. Li, Z. Zhang, D. Psaltis, A. Scherer, *Appl. Phys. Lett.* **2007**, *91*, 051109.
[8] D. O'Carroll, I. Lieberwirth, G. Redmond, *Nat. Nanotechnol.* **2007**, *2*, 180.
[9] M. Steinhart, J. H. Wendorff, A. Greiner, R. B. Wehrspohn, K. Nielsch, J. Schilling, J. Choi, U. Gösele, *Science* **2002**, *296*, 1997.
[10] J. M. Moran-Mirabal, J. D. Slinker, J. A. DeFranco, S. S. Verbridge, R. Ilic, S. Flores-Torres, H. Abrua, G. G. Malliaras, H. G. Craighead, *Nano Lett.* **2007**, *7*, 458.
[11] E. Mele, F. Di Benedetto, L. Persano, R. Cingolani, D. Pisignano, *Nano Lett.* **2005**, *5*, 1915.
[12] K. C. Hui, J. An, X. Y. Zhang, J. B. Xu, J. Y. Dai, H. C. Ong, *Adv. Mater.* **2005**, *17*, 1960.
[13] D. Kan, T. Terashima, R. Kanda, A. Masuno, K. Tanaka, S. Chu, H. Kan, A. Ishizumi, Y. Kanemitsu, Y. Shimakawa, M. Takano, *Nat. Mater.* **2005**, *4*, 816.
[14] M. C. Gupta, A. Gupta, J. Horwitz, D. Kliger, *Macromolecules* **1982**, *15*, 1372.
[15] S. O. Cho, E. J. Lee, H. M. Lee, J. G. Kim, Y. J. Kim, *Adv. Mater.* **2006**, *18*, 60.
[16] J. Robertson, *Mater. Sci. Eng. R* **2002**, *37*, 129.
[17] M. Füle, S. Tóth, M. Veres, I. Pócsik, M. Koós, *Diamond Relat. Mater.* **2005**, *14*, 1041.
[18] Ma. Esther Martínez-Pardo, J. Cardoso, H. Vázquez, M. Aguilar, J. Rickards, E. Andrade, *Nucl. Instrum. Methods Phys. Res. Sect. B* **1997**, *131*, 219.
[19] N. I. Nijegorodov, W. S. Downey, *J. Phys. Chem.* **1994**, *98*, 5639.
[20] B. K. Gan, M. M. M. Bilek, A. Kondyurin, K. Mizuno, D. R. McKenzie, *Nucl. Instrum. Methods Phys. Res. Sect. B* **2006**, *247*, 254.
[21] Y. H. Ye, S. Badilescu, Vo-Van Truong, P. Rochon, A. Natansohn, *Appl. Phys. Lett.* **2001**, *79*, 872.
[22] A. D. Peng, E. B. Xiao, Y. Ma, W. S. Yang, J. N. Yao, *Adv. Mater.* **2005**, *17*, 2070.
[23] S. O. Kim, H. H. Solak, M. P. Stoykovich, N. J. Ferrier, J. J. de Pablo, P. F. Nealey, *Nature* **2003**, *424*, 411.
[24] M. P. Stoykovich, M. Müller, S. O. Kim, H. H. Solak, E. W. Edwards, J. J. de Pablo, P. F. Nealey, *Science* **2005**, *308*, 1442.
[25] S. O. Cho, H. Y. Jun, S. K. Ahn, *Adv. Mater.* **2005**, *17*, 120.
[26] F. J. Hohn, *J. Vac. Sci. Technol. J. B* **1989**, *7*, 1405.
[27] M. F. Ng, S. L. Sun, R. Q. Zhang, *J. Appl. Phys.* **2005**, *97*, 103513.